ISSN: 2643-6876
DOI: 10.33552/CTCSE.2026.12.000784
Current Trends in
Civil & Structural Engineering
Iris Publishers

Review Article

Compressive Relaxation in Concrete

Pierre Rossi*

Civil Engineering Department, COPPE, Federal University of Rio de Janeiro, Brazil

***Corresponding author:** Pierre Rossi, Civil Engineering Department, COPPE, Federal University of Rio de Janeiro, Brazil

Received Date: May 18, 2025
Published Date: May 28, 2025

Abstract

For the general purpose of analyzing the physical mechanisms underlying the delayed behavior of concrete and achieving a suitable modeling approach, this article presents the development of a compression relaxation test. Following a literature review, the chosen strategy was to adapt the testing frame for creep tests. The test was then used to conduct an initial experimental study. This study confirms that the use of a linear viscoelastic model for the basic creep and relaxation of concrete is appropriate. The article also provides a critical analysis of current early-age concrete cracking models, highlighting their lack of physical relevance.

Keywords: Concrete; Creep; Relaxation; Compression; Linear Viscoelacity; Cracking Models; Early Age

Introduction

Modeling the time-dependent behavior of concrete structures is of major importance, particularly for prestressed structures and concrete behavior at early age. Most mechanical models developed to date rely on linear viscoelasticity and use the superposition principle. For these models, practically only creep tests are needed and performed, since relaxation is considered, from a mathematical standpoint, as the dual of creep. However, the literature has not yet experimentally demonstrated that linear viscoelasticity is the best theory for modeling the time-dependent behavior of concrete. One approach to assess the relevance of using linear viscoelasticity for concrete is to perform creep and relaxation tests in parallel on the same concrete in order to analyze whether one is indeed the dual of the other. Regarding relaxation tests, the literature review conducted has highlighted the lack of satisfactory solutions. So: (1) Fairbairn et al. [1] developed a relaxation test with manual deformation control, which led to unreliable results. (2) Ring tests on early-age concrete have been carried out [2-4]. These are indirect tensile relaxation tests. They provide information that is highly dependent on the analysis model used for this type of indirect test. (3) Compression relaxation tests have been conducted using hydraulic presses [5, 6]. Due to the use of such experimental equipment, the test duration can only be very short and therefore very incomplete. Moreover, maintaining a constant deformation with a hydraulic press leads to temperature increases that disturb the test [4]. In this study, an experimental setup is proposed consisting of adapting an existing creep frame. This creep frame maintains a constant pressure in a hydraulic jack (and therefore a constant load in the specimen) using an oleopneumatic (nitrogen/oil) pressure accumulator. The proposed adaptation is based on the principle of a controlled leakage of pressurized nitrogen contained in an oleopneumatic accumulator, in order to reduce the load in the specimen so as to maintain a constant length. The load evolution is determined by measuring the hydraulic pressure in the loading jack (Figure 1). The use of a low-pressure electropneumatic servovalve combined with a high-pressure relief valve allows controlling the leakage. This paper presents, on the one hand, the equipment and the proposed test procedure well as the first experimental result obtained. More importantly (and this is the main originality of the present paper), it provides a detailed analysis of the physical mechanisms underlying compressive stress relaxation in concrete. This analysis contradicts the approach generally adopted at the international level, which considers that stress relaxation in concrete reduces the risk of cracking. This creep frame maintains a constant pressure in a hydraulic jack (and therefore a constant load in the specimen) using an oleopneumatic (nitrogen/oil) pressure accumulator.

The proposed adaptation is based on the principle of a controlled leakage of pressurized nitrogen contained in an oleopneumatic accumulator, in order to reduce the load in the specimen so as to maintain a constant length. The load evolution is determined by measuring the hydraulic pressure in the loading jack. The use of a low-pressure electropneumatic servovalve combined with a high-pressure relief valve allows controlling the leakage. This paper presents, on the one hand, the equipment and the proposed test procedure well as the first experimental result obtained. More importantly (and this is the main originality of the present paper), it provides a detailed analysis of the physical mechanisms underlying compressive stress relaxation in concrete. This analysis contradicts the approach generally adopted at the international level, which considers that stress relaxation in concrete reduces the risk of cracking.

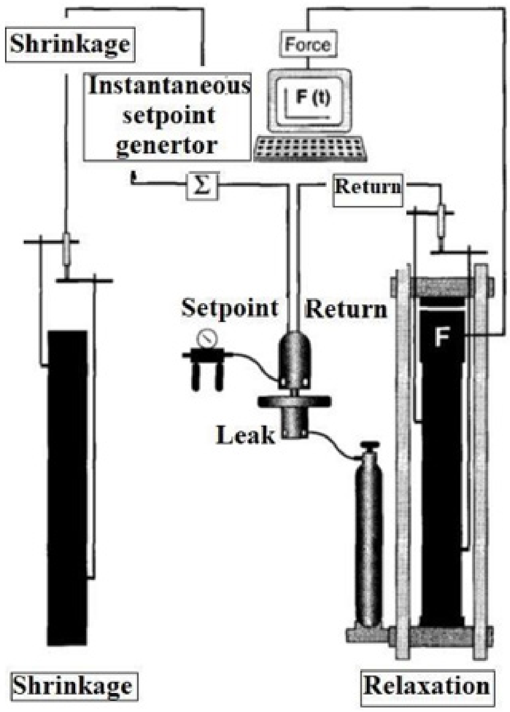

Figure 1: Schematic presentation of the experimental setup for the relaxation test.

Operation of the servopilot and relief system

The electropneumatic servopilot associated with the relief valve is connected to the filling valve of the accumulator. As in any feedback-controlled system, a controlled (or feedback) electrical signal is forced to follow a command (or setpoint) signal. This controlled signal is proportional to the deformation of the specimen. The comparison between these two signals is performed in the Proportional-Integral-Derivative (PID) controller integrated into the electropneumatic servovalve. This controller adjusts the response of the control system. The servopilot therefore includes two stages (Figure 2): the PID regulation loop and the electropneumatic converter. Two solenoid valves (inlet and exhaust) regulate the output pressure of the converter using the compressed-air network. The controlled pneumatic output of the converter acts on the relief valve command through a diaphragm-type pressure amplifier. This enables the control of high upstream pressures thanks to a higher actuation ratio. The applied pneumatic amplification ratio is 31.75. A relief valve regulates the upstream pressure, unlike pressure reducers, which regulate a downstream pressure. They are designed to keep constant any physical quantity related to a pressure - in this case, a compressive deformation (their action is similar to a safety valve, but with better regulation and higher sensitivity). Since the oil pressure in the oleopneumatic accumulator equals the nitrogen pressure, the drop in load in the specimen is controlled so as to maintain its deformation constant.

Citation: Pierre Rossi*. Compressive Relaxation in Concrete. Cur Trends Civil & Struct Eng. 12(3): 2026. CTCSE.MS.ID.000784.
DOI: 10.33552/CTCSE.2026.12.000784.

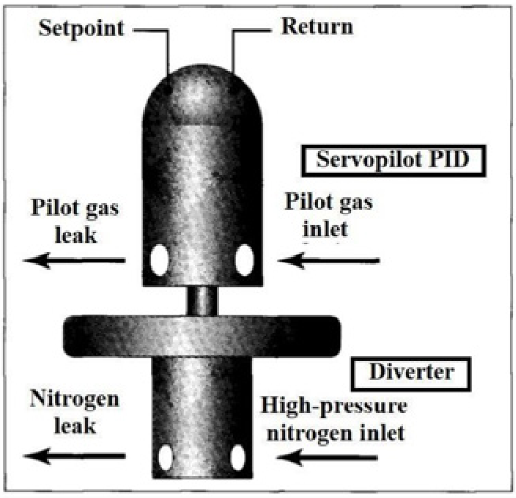

Figure 2: Details of the device (servopilot and diverter).

Setpoint and feedback

The setpoint and the feedback are applied to the PID controller. The feedback originates from a ±1 mm differential transformer displacement sensor measuring the deformations of the relaxation specimen (A base length of 500 mm is used to electronically determine the strain). The setpoint of a relaxation test is a constant initial imposed deformation throughout the test, $\varepsilon_0(t_0)$. It corresponds to an initial stress $\sigma_0(t_0)$, and the evolution of stress as a function of time, σ(t), is recorded. However, it is known that in addition to viscous strains ε^v, concrete may undergo shrinkage strains ε^{sh} (Θ, HR, μ) of thermal (Θ), hygrometric (HR), and autogenous (μ) origin. In the case of the time-dependent behavior of concrete, the incremental expression of the stress evolution is:

$$d\sigma = E\left(d\varepsilon - d\varepsilon^{sh} - d\varepsilon^{v}\right) \quad (1)$$

where dε is the total strain increment measurable under imposed stress or imposable under imposed strain. The objective of a relaxation test is to measure:

$$d\sigma = -E\, d\varepsilon^{v} \quad (2)$$

Therefore, it is necessary that:

$$d\sigma = d\varepsilon^{sh} = d\varepsilon^{imp} \quad (3)$$

The setpoint imposed during the relaxation test is then expressed as:

$$\varepsilon^{imp} = \varepsilon_0\left(t_0\right) + \int d\varepsilon^{sh} \quad (4)$$

A relaxation test is therefore associated with a load-free companion specimen (Figure 3), used to measure $\varepsilon^{sh}(t)$. This measurement is added to the constant setpoint representing the initial deformation $\varepsilon_0(t_0)$.

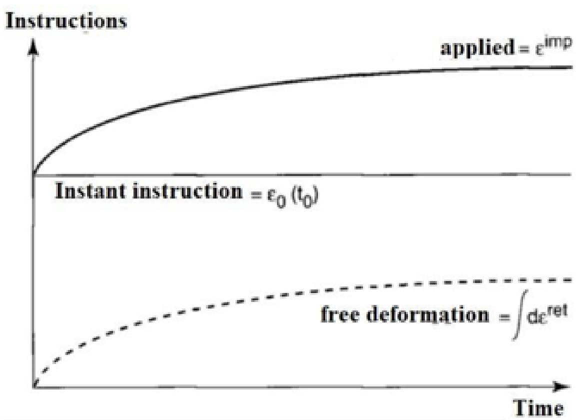

Figure 3: Diagram explaining the generation of the instruction set.

Application of the instantaneous deformation

Initially, the nitrogen pressure is set to a value corresponding to a load slightly higher than the one required to produce the target deformation, but the accumulator is isolated from the loading jack. The setpoint is defined at the deformation value corresponding to the estimated initial deformation (free-deformation variations may be neglected during the loading phase). This estimate may be refined using a preliminary compression test on a specimen from the same concrete. The loading consists of connecting the accumulator to the loading jack. The excess load is very rapidly released by the control system (Figure 4).

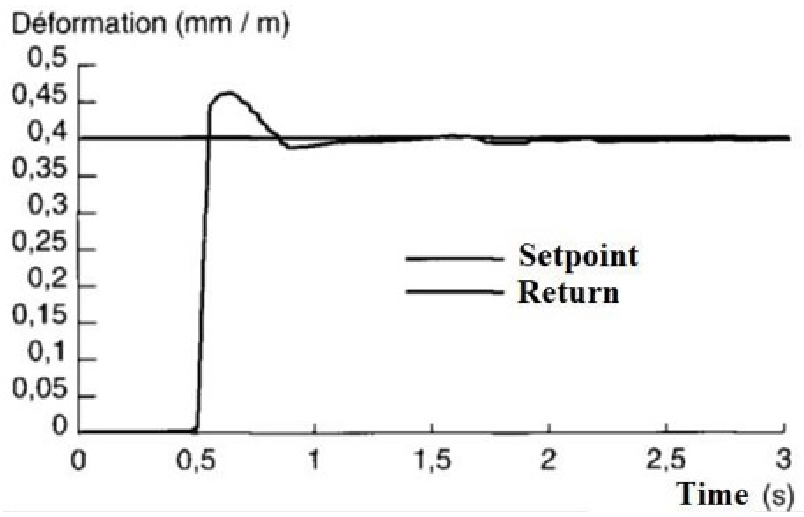

Figure 4: Load control response.

Remarks regarding the setup phase

The overall calibration of the experimental device is delicate because the servopilot is primarily designed for operation as a pressure reducer and not as a relief valve, which means that the PID tuning modes are very different and had to be adapted to the present application. This phase also allows defining sensor quality and data acquisition requirements. A direct force measurement is used. The loading jack is a low-profile jack without seals, with an effective surface area that varies with its stroke. The force sensor must be accurate and have a reliable long-term response without creep. Including a force sensor in series with the specimen requires reducing the specimen height compared to the creep test (Figure 1). Its height was reduced from 100 to 85 cm (for a diameter of 16 cm).

First experimental result

Concrete tested

The mix design of the tested concrete is given in Table 1

Table 1: Mix design of the concrete.

Constituent	kg/m^3
Sand 0/4	424
Sand 0/5	431
Gravel 5/12.5	454
Gravel 12.5/20	540
Cement CEM I 52.5 R	350
Water	180

Creep, shrinkage, and relaxation tests are carried out in parallel at a concrete age of 28 days. At this age, the compressive strength of the concrete is 38 MPa and its Young's modulus is 30 GPa.

This first relaxation test is fully controlled, fully automatic, and autonomous. As in the creep test, the loading is instantaneous (less than 0.5s) and the deformation is controlled with micrometer precision. The compressive stress applied for the creep test represents 30% of the concrete comressive strength and the deformation applied for the relaxation test is in relation with this creep loading (considering the concrete Young modulus). All specimens tested (for creep, relaxation, and shrinkage) are protected (throughout the entire test) from desiccation using a double layer of self-adhesive aluminum foil. Thus, the creep test is a basic creep test, the shrinkage test is an autogenous shrinkage test, and the relaxation test is a basic relaxation test. It is important to stress that creep and shrinkage tests have long been fully mastered and have been the subject of numerous publications in which they are described in detail (Among them [7–10] can be considered).

Experimental result and analysis of the relaxation test

The curve in Figure 5 compares the experimental results with a calculation performed within the framework of non-aging linear viscoelasticity. A Kelvin–Voigt model was first fitted to the results of the basic creep test. For both tests, shrinkage deformation was subtracted. Using this model and applying Carson transforms [11], the corresponding relaxation function was determined. It appears that, over a 13-day time interval (duration of the tests), the relaxation test and the model give consistent results.

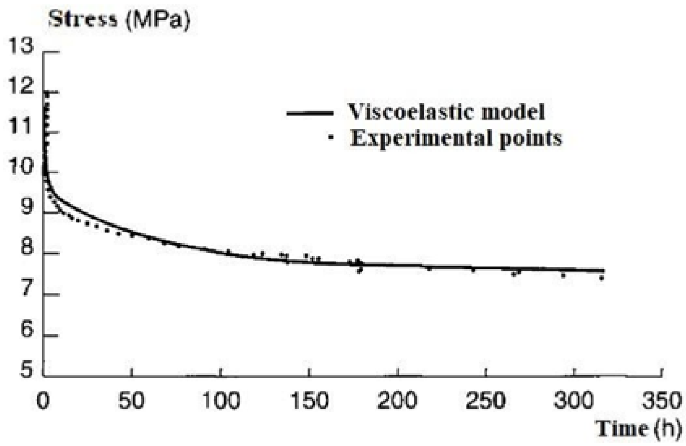

Figure 5: Experimental results compared to calculations (viscoelastic model).

Analysis and consequences related to the experimental study

The results of this first experimental study show that the use of linear viscoelasticity is relevant for modeling the basic creep and stress relaxation of concrete in compression. It can therefore be considered that relaxation is the mechanical dual of creep. This confirmation has an important physical consequence. Indeed, it is reasonable to assume and to propose that the physical mechanisms governing these two mechanical behaviors are identical. Yet previous experimental studies [7–10] have clearly demonstrated that the physical origin of basic creep in concrete is linked to couplings between microcracking in the material and the water and vapor transfers induced by this microcracking. These couplings generate an additional autogenous shrinkage within the material. In other words, if there is no microcracking, there is no basic creep. Based on what has been stated above, it can also be considered that if there is no microcracking, there is likewise no basic stress relaxation in concrete.

However, it is accepted that tensile stress relaxation in concrete leads to a reduction in its tendency to crack (in particular through the numerical models developed to date). This consideration is, in fact, incorrect in light of the work presented in this article, since stress relaxation cannot occur without microcracking - tensile stresses being the very cause of concrete cracking. This is all the truer since it has been experimentally shown that basic creep in tension (and therefore basic relaxation) is less significant than basic creep in compression [5, 6] - again, because tensile stresses are the origin of concrete cracking. The question is therefore to understand why most numerical models must introduce tensile stress relaxation in concrete in order to correctly simulate the cracking process.

The answer proposed in this article is the following: all numerical cracking models - whether they belong to the fictitious (or cohesive) crack family models [12-15] or to the diffused crack family models (such as crack band models, smeared crack models or damage models [16-27]) - are physically unfounded. Indeed, all of these models use the fracture energy G_f, as the main cracking parameter of the material. However, fracture energy G_f is not an intrinsic property of concrete, because it depends on the size of the laboratory specimen used to determine it [28–38]. The only material parameter related to cracking that is truly intrinsic is the critical energy release rate, G_c. This parameter is used in the framework of linear elastic fracture mechanics (LEFM). Moreover, G_c is always greater than G_f (G_f equals G_c only when determined from very large specimens, which are rarely tested in laboratories).

DOI: 10.33552/CTCSE.2026.12.000784.

It then becomes clear that if, in a numerical cracking model, G_f is lower than G_c - the actual measure of the material's resistance to cracking - it becomes necessary to artificially reduce the tensile stresses within the material (the driving force of cracking) by relaxing them. The issue with this compensatory approach is determining how much tensile stress must be relaxed (for example by introducing linear viscoelasticity into the numerical model) given the value of G_f adopted to analyze the cracking of the structure under consideration. Since G_f is determined from a specimen whose dimensions may be very different from those of the actual structure, achieving predictive numerical simulation becomes extremely challenging. It is interesting to point out that, more recently, a semi-explicit cracking model was developed and validated with success using the parameter G_c [39, 40]. The basis of extension of this model has been recently proposed [41] for analyzing the early age cracking process of concrete structures. This extension does not consider a relaxation of the tensile stresses.

Conclusions

This paper presents the development of a compression relaxation test. This test is an adaptation of a testing frame previously developed and used for creep tests. It is used to conduct an initial experimental study. This study shows that the relaxation is the mechanical dual of creep and, so, confirms that the use of a linear viscoelastic model for the basic creep and relaxation of concrete is appropriate. The article provides also a critical analysis of current early-age concrete cracking models and highlighs their lack of physical relevance.

Acknowledgments

None.

Conflict of Interest

No conflict of interest.

References

1. Fairbairn EMR, Timsah Y, Menezes NC (1993) A comparison between experimental and numerical data for concrete subjected to variable strains, Creep and Shrinkage. ZP Bazant, I Carol Published by E & FN Spon.
2. Gao Y, Zhang J, Han P (2013) Determination of stress relaxation parameters of concrete in tension at early-age by ring test, Construction and Building Materials 41: 152164.
3. Hossain AB, Weiss J (2004) Assessing residual stress development and stress relaxation in restrained concrete ring specimens, Cement and Concrete Composites 26(5): 531-540.
4. Shen D, Liu K Ji Y, Shi H, Zhang J (2018) Early-age residual stress and stress relaxation of high-performance concrete containing fly ash, Magazine of Concrete Research 70(14): 726–738.
5. Taylor MA, Maurer GK (1973) Short-term stress relaxation of concrete, Magazine of Concrete Research 25(84):123–135.
6. Hamed E (2016) Relaxation Behavior of Concrete under Sustained Uniaxial Compressive Deformation. Journal of Materials in Civil Engineering 28(6).
7. Rossi P, Godart B, Robert JL, Gervais JP, Bruhat D (1994) Investigation of basic creep of concrete by acoustic emission technics. Materials and Structures 27: 510-514.
8. Rossi P, Tailhan JL, Le Maou F, Gaillet L, Martin E (2012) Basic creep behavior of concretes investigation of the physical mechanisms by using acoustic emission. Cement and Concrete Research 42(1): 61-73.
9. Tailhan JL, Boulay C, Rossi P, Le Maou F, Martin E (2012) Compressive, tensile and bending basic creep behaviours related to the same concrete, Structural Concrete 14(2): 124-130.
10. Rossi P, Tailhan JL, Le Maou F (2013) Comparison between concrete creeps in tension and in compression: influence of the concrete age at the loading and of the drying conditions, Cement and Concrete Research 51: 78-84.
11. Salençon J (1983) Viscoélasticité, presses de l'ENPC (in french).
12. Hillerborg A, Modeer M, Petersson P (1976) Analysis of crack formation and crack growth in concrete by means of fracture mechanics and finite elements. Cem Concr Res 6: 773–782.
13. Hillerborg A (1085) Numerical methods to simulate softening and fracture of concrete, In Fracture Mechanics of Concrete: Structural Application and Numerical Calculation; Springer: Dordrecht, The Netherlands pp. 141–170.
14. Barros J, Figueiras JA (2001) Model for the analysis of steel fiber reinforced concrete slabs on grade. Computers & Structures 79(1): 97-106.
15. Cunha V, Barros J, Sena-Cruz J (2012) A finite element model with discrete embedded elements for fiber reinforced composites. Computers & Structures 94-95: 22-33.
16. Bazant ZP, Oh BH (1983) Crack band theory for fracture of concrete, Matériaux Constr. 9(16): 155–177.
17. Mazars J (1984) Application de la mécanique de l'endommagement au comportement nonlinéaire et la rupture du béton de structure, Ph.D. thesis LMT (in french).
18. Rots J, Nauta P, Kuster G, Blaauwendraad J (1985) Smeared crack approach and fracture localization in concrete, HERON 30(1).
19. Pijaudier Gabot G, Bazant ZP (1987) Nonlocal damage theory. J Eng Mech ASCE 113: 1512-1533.
20. Jirasek M, Zimmermann T (1998) Rotating crack model with transition to scalar damage. Journal of engineering mechanics 124(3): 277–284.
21. Bazant Z, Jirasek M (2002) Nonlocal integral formulations of plasticity and damage: survey of progress. J Eng Mech 128: 1119-1149.
22. Oliver J, Huespe AE, Samaniego E, Chaves E (2004) Continuum approach to the numerical simulation of material failure in concrete. International journal for numerical and analytical methods in geomechanics 28 (7-8): 609–632.
23. Oliver J, Huespe AE (2004) Continuum approach to material failure in strong discontinuity settings, Computer methods in applied mechanics and engineering 193 (30-32): 3195–3220.
24. Fanella D, Krajcinovic D (1985) Continuum damage mechanics of fiber reinforced concrete. J Eng Mech 111(8): 995-1009.
25. Li F, Li Z (2000) Continuum damage mechanics-based modeling of fiber reinforced concrete in tension. Int J Solids Struct 38: 777-793.
26. Peng X, Meyer C (2000) A continuum damage mechanics model for concrete reinforced with randomly distributed short fibers, Comput Struct 78: 505-515.
27. De Montaignac R, Massicotte B, Charron JP (2013) Finite-element modelling of SFRC members in bending. Magazine of Concrete Research 65(19): 1133-1146.
28. Hillerborg A, Modéer M, Petersson PE (1976) Analysis of crack formation and crack growth in concrete by means of fracture mechanics and finite elements, Cement and concrete research 6: 773–781.
29. Entov VM, Yagust VY (1975) Experimental investigation of laws governing quasi-static development of crack in concrete. I 2V. AN. SSSR. Mekhnica, Tvergo, Tela 10(4): 93-103.

30. Watson RL (1978) The estimation of fracture energy as a measure of toughness of hardened cement paste. Cement and Concrete Research 8: 651-556.

31. Wittman FH (1981) Mechanismes and mechanics of fracture of concrete. I.C.F.5 Cannes 4: 1467-1487.

32. Walsh PF (1982) Fracture of plain concrete. Indian Concrete Journal pp 469-476.

33. Carpinteri A (1982) Experimental determination of fracture toughness KIC for aggregative materials. Advances in Fracture research (fracture 81), D. François, Pergamon Press, Oxford 4: 1491-1498.

34. Shah SP (1984) Application of fracture mechanics to cementitious materials. Preprints of the proceedings NATO Advanced Workshop. Northwestern University, Evanston, USA.

35. Reinhardt HW (1986) The role of fracture mechanics in rational rules for concrete design. IABSE RERIODICA 1.

36. Rossi P, Acker P, Francois D (1984) Measurements of the Fracture Toughness KIC of Concrete. Proceeding of the 6th International Conference on Fracture, New Delhi, pp. 2839.

37. Rossi P. et al. (1991) Fracture properties of concrete determined by means of wedge splitting tests and tapered double cantilever beams tests. Fracture mechanics test methods for concrete. RILEM report 5, Shah S, Carpinteri A (Eds.), Chapman and Hall, CRC Press.

38. Rossi P et al. (2022) Comparison between plain concrete toughness and steel fibre reinforced concrete toughness. Cement and Concrete Research 16: 303-313.

39. Rita MR (2022) Implementation of a macroscopic probabilistic model of cracking concrete using parallelization strategies. PhD Thesis of Federal University of Rio de Janeiro.

40. Rita MR, Rossi P, Fairbairn EdMR, Ribeiro FLB (2024) Determination of the Probabilistic Properties of the Critical Fracture Energy of Concrete Integrating Scale Effect Aspects. Appl Sci 2024(14): 462.

41. Rossi P (2025) Cracking Process of Early-Age Concretes: Basis of Numerical Probabilistic Models. Buildings 15: 2259.